

6. T. Yagi and T. Hishinuma, *Geophys. Res. Lett.* **22**, 1933 (1995).
7. T. Hishinuma, T. Yagi, T. Uchida, *Proc. Jpn. Acad.* **70B**, 71 (1994).
8. The settling time of the droplets depends on the viscosity of the silicate melt. For the experiment of long duration at high temperature, the amount of H₂O in the starting material should be reduced to make the settling time longer to prevent interaction between the droplets and the capsule wall. In the experiments with various amounts of H₂O in the capsule, comparison of the H concentration in FeHx measured in this study is less meaningful to confirm the equilibrium because it depends on $a_{\text{H}_2\text{O}}$ in the silicate melt. Comparison of the equilibrium constant K rather than the H concentration in FeHx is more suitable to confirm the equilibrium of reaction 2. The value of K at 1200°C and at 1500°C shows little variation despite various run durations (Table 1).
9. Y. Fukai and H. Sugimoto, *Adv. Physics* **34**, 263 (1985).
10. Y. Fukai, *Nature* **308**, 174 (1984).
11. J. V. Badding, R. J. Hemley, H. K. Mao, *Science* **253**, 421 (1991).
12. M. Yamakata, T. Yagi, W. Utsumi, Y. Fukai, *Proc. Jpn. Acad.* **68B**, 172 (1992).
13. Y. Fukai and S. Akimoto, *ibid.* **59B**, 158 (1983).
14. T. Inoue and H. Sawamoto, in *High-Pressure Research: Application to Earth and Planetary Sciences*, Y. Syono and M. H. Manghnani, Eds. (Terra Scientific Publishing Company/American Geophysical Union, Tokyo/Washington, DC, 1992), pp. 323–331. The $K_{\text{Fe}^{2+}/\text{Fe}^{3+}}^{\text{Mg/Fe}}$ was calculated from the composition of the coexisting olivine and hydrous silicate melt reported here.
15. Y. Fukai, *Jpn. J. Appl. Phys.* **22**, 207 (1983).
16. A. Suzuki, E. Ohtani, T. Kato, *Science* **269**, 216 (1995).
17. E. Stolper, *Geochim. Cosmochim. Acta* **46**, 2609 (1982).
18. T. Inoue, *Phys. Earth Planet. Inter.* **85**, 237 (1994).
19. Reaction 2 can be rewritten with the FeO component in an ideal solution of oxides instead of Fe²⁺ and O²⁻ in the silicate melt. This approach yields $\Delta H^\circ = 136 \pm 27$ kJ/mol, which is almost identical to the value reported here.
20. A. E. Ringwood, *Geochem. J.* **11**, 111 (1977).
21. L. Grossman and J. W. Larimer, *Rev. Geophys. Space Phys.* **12**, 71 (1974).
22. Y. Fukai and T. Suzuki, *J. Geophys. Res.* **91**, 9222 (1986). In this paper, a detailed mass-balance calculation for estimating the core composition was done with the two-component model (20) for Earth's bulk inventory of the light elements.
23. E. Takahashi, *J. Geophys. Res.* **91**, 9367 (1986).
24. D. J. Stevenson, in *Origin of the Earth*, H. E. Newsom and J. H. Jones, Eds. (Oxford Univ. Press, New York, 1990), pp. 231–249.
25. Y. Abe and T. Matsui, *J. Geophys. Res.* **90**, C545 (1985); *ibid.* **91**, E291 (1986).
26. Y. Fukai, in *High-Pressure Research: Application to Earth and Planetary Sciences*, Y. Syono and M. H. Manghnani, Eds. (Terra Scientific Publishing Company/American Geophysical Union, Tokyo/Washington, DC, 1992), pp. 373–385.
27. ———, *Kagaku* **54**, 36 (1984) (in Japanese).
28. D. J. Stevenson, *Nature* **268**, 130 (1977); *Science* **214**, 611 (1981).
29. The author thanks E. Takahashi for discussion and criticism, for reading and correcting this report, and for help and advice in the high-pressure experiments. Critical reviews by two anonymous referees improved this manuscript very much. Supported by the Foundation for Research Fellowships of Japan Society for the Promotion of Science for Young Scientists (DC1). Contribution 17 from the Magma Factory.

21 April 1997; accepted 20 October 1997

Correlations Between Ground and Excited State Spectra of a Quantum Dot

D. R. Stewart, D. Sprinzak, C. M. Marcus,* C. I. Duruöz, J. S. Harris Jr.

The ground and excited state spectra of a semiconductor quantum dot with successive electron occupancy were studied with linear and nonlinear magnetoconductance measurements. A direct correlation was observed between the m th excited state of the N -electron system and the ground state of the $(N + m)$ -electron system for m up to 4. The results are consistent with a single-particle picture in which a fixed spectrum of energy levels is successively filled, except for a notable absence of spin degeneracy. Further departures from the single-particle picture due to electron-electron interaction were also observed. Magnetoconductance fluctuations of ground states show anti-crossings where wave function characteristics are exchanged between adjacent levels.

Quantum dots (QDs) are small electrically conducting regions, typically 1 μm or less in size, containing from one to a few thousand electrons (1). Because of the small volume, the allowed electron energies within the dot are quantized, forming a discrete spectrum of quantum states, not unlike the energy levels of an atom. However, in contrast to the ordered shell structure of atomic spectra—a consequence of the spherically symmetric potential that binds the electrons—the generic energy spectrum of a QD (lacking any special symmetry) shows

no shell structure, but instead has universal statistical properties associated with the underlying universality of quantum chaos (2).

Disordered or irregularly shaped QDs are examples of so-called mesoscopic systems—small electronic structures intermediate in size between atoms and macroscopic (classical) objects that have universal spectral and transport properties that are independent of material, shape, or disorder. In the past few years, a remarkable set of connections between mesoscopic systems, complex quantum systems such as heavy nuclei (where the statistical approach to spectra was first developed), quantum systems whose classical analogs are chaotic, and random matrix theory has emerged, providing deep theoretical insight into the generic properties of quantum systems (2). These connections are based principally on noninteracting, single-particle spectral properties; only recently has attention been focused on mesoscopic systems in which interactions between particles and quantum interference play equally im-

portant roles. It is in this context that the generic spectral features of multi-electron QDs are of great interest.

The electronic spectra of QDs are governed by the interplay of two energy scales: the Coulomb interaction or charging energy associated with adding a single electron to the dot, and the confinement energy associated with quantization due to the confining potential. In lateral semiconductor QDs the charging energy is typically an order of magnitude larger than the quantum confinement energy, which suggests that the quantum spectrum of the $(N + 1)$ -electron QD may be uncorrelated with the spectrum of the N -electron QD (1). On the other hand, in recent theoretical work (3) it has been argued that modifications to the universal single-particle spectrum resulting from electron-electron interactions should be smaller than, or at most comparable with, the typical energy spacing between quantum levels, suggesting that spectra for successive N may remain correlated.

Previous investigation of QD spectra by transport and capacitance spectroscopy has concentrated on analysis of the “addition” energy spectrum composed of the ground states of the QD for successive numbers of electrons (1, 4–6). Several experiments (7–10) have also probed the “excitation” spectrum of quantum levels in the QD for fixed electron numbers using nonlinear conductance measurements. These measurements showed spectral features attributed to electron-electron interactions such as spin blockade (9) and clusters of resonances identified with a single excited state (10). Many-body calculations for few-electron systems ($N \leq 5$) have explained some of the experimentally observed features in terms of spin and spatial selection rules (11), spectrally dominant center-of-mass excitation modes

D. R. Stewart, Department of Applied Physics, Stanford University, Stanford, CA 94305, USA.

D. Sprinzak, Department of Physics, Stanford University, Stanford, CA 94305, USA, and Braun Center for Submicron Research, Department of Condensed Matter Physics, Weizmann Institute of Science, Rehovot 76100, Israel.

C. M. Marcus, Department of Physics, Stanford University, Stanford, CA 94305, USA.

C. I. Duruöz and J. S. Harris Jr., Department of Electrical Engineering, Stanford University, Stanford, CA 94305, USA.

*To whom correspondence should be addressed.

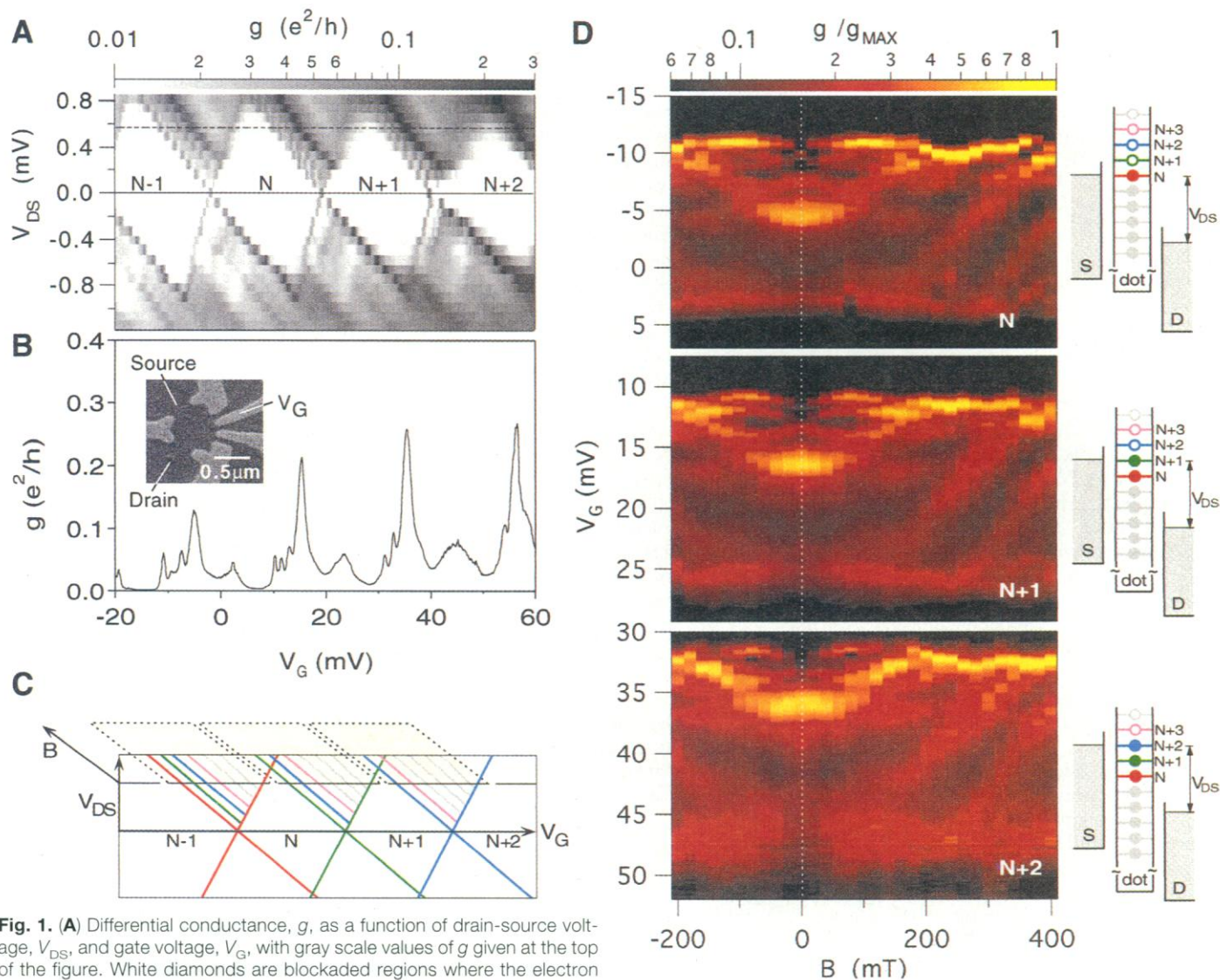


Fig. 1. (A) Differential conductance, g , as a function of drain-source voltage, V_{DS} , and gate voltage, V_G , with gray scale values of g given at the top of the figure. White diamonds are blocked regions where the electron number is fixed. Dark diagonal stripes (peaks) parallel to the diamond edges correspond to QD levels in resonance with the source or drain Fermi levels. Magnetic field $B = 30$ mT. (B) One trace from (A) at $V_{DS} = 0.57$ mV [dotted line in (A)]. The distinctive high peak appears as the second resonance from the left (first excited state) in the rightmost CB peak and shifts to the third, fourth, and fifth (not resolvable) resonance (second, third, and fourth excited states) as the electron number decreases. Decreasing average g is attributed to capacitive coupling between V_G and adjacent gates. (Inset) Scanning electron micrograph of the QD studied. (C) Coulomb diamond schematic, with colored stripes corresponding to different quantum levels in the dot. Yellow planes correspond to the data in (D). Stripes parallel to the positive slope edge of the Coulomb diamonds are not shown because they were not resolved in the experiment. (D) The

broadened CB peaks shown in (B) as a function of B . The color scale of g of each spectrum is normalized to the maximum g (g_{MAX}) of that spectrum (given at the top of the figure). The resonance pattern of each CB peak corresponds to the excitation spectrum of the N , $(N + 1)$, or $(N + 2)$ electron QD. As each electron is removed, a new resonance is introduced and the rest of the spectrum shifts by one level. To the right are energy diagrams for N , $(N + 1)$, or $(N + 2)$ electrons in the QD with filled circles indicating occupied levels and colors corresponding to (C). Diagrams show the position of QD levels for the topmost (ground state) feature in each broadened peak where the N , $(N + 1)$, or $(N + 2)$ levels are in resonance with the source Fermi level. Higher levels (open circles) are brought into resonance by lowering the dot potential [making V_G more positive in (D)].

(12), and nonequilibrium effects (13). Very recently, ground and excited state spectra were both investigated in a circular, few electron QD (14).

We present an experimental study of correlations between ground state addition spectra and excitation spectra of an irregularly shaped QD containing several hundred electrons. We found that excitation and addition spectra for successive electron occupancies are remarkably correlated, re-

sembling in many respects a noninteracting picture in which electrons simply fill the excited states, so that addition and excitation spectra coincide. Departures from this single-particle model were also observed, giving insight into the electron-electron interaction strength. Additionally, we observed that spin degeneracy appears to be absent in the QD spectrum.

Measurements were performed on a QD defined by applying ~ -0.3 V to Cr-Au

electrostatic gates on the surface of a GaAs-AlGaAs heterostructure (inset, Fig. 1B), depleting a two-dimensional electron gas (2DEG) 900 Å below the surface. The ungated 2DEG mobility and density were 1.4×10^5 cm²/V·s and 2.0×10^{11} cm⁻² at 4.2 K. We measured the differential conductance $g = dI/dV_{DS}$ (I is current) of the QD in the Coulomb blockade (CB) regime (1) in a dilution refrigerator using ac lock-in techniques with a 6- μ V ac excitation

added to a dc bias in the range of ± 1.5 mV. Measurements were made as a function of gate voltage (V_G), drain-source dc bias (V_{DS}), and magnetic field (B) applied perpendicular to the 2DEG plane. The experimental gate voltage was scaled to dot energy by using both the nonlinear CB peak width ($\sim eV_{DS} + 3.5k_B T$, where e is electronic charge, k_B is Boltzmann's constant, and T is temperature) at finite V_{DS} and independently by a fit of CB peak widths at $V_{DS} = 0$ as a function of temperature (15). The electron temperature in the dot was 90 ± 10 mK ($k_B T \sim 8 \mu\text{eV}$) as determined from the full width at half maximum of linear CB peaks. The mean energy level spacing in the dot measured from the excited state spectra (discussed below) was $\Delta \sim 35 \mu\text{eV}$, providing an estimate of the dot area, $A = \pi \hbar^2 / m^* \Delta \sim 0.1 \mu\text{m}^2$ [m^* is the electron effective mass in GaAs and \hbar is Planck's constant (h) divided by 2π]. This area is consistent with the lithographic area allowing ~ 150 nm for lateral depletion and yields an occupancy of electrons in the dot of $N \sim 200$. All magnetoconductance measurements were performed in the regime $g < 0.3 e^2/h$, and in the regime of single-electron transport, that is, $0 < |eV_{DS}| < E_C$, where $E_C \sim 730 \mu\text{eV}$ is the classical charging energy of the QD measured from linear CB peak spacings.

A typical nonlinear differential conductance measurement through the QD as a function of V_G and V_{DS} is shown in Fig. 1A. At $V_{DS} = 0$ the familiar CB peaks can be seen, roughly equally spaced in V_G . Increasing V_{DS} results in broadening of the CB peaks to form multiple peak structures (7, 8) enclosing so-called "Coulomb diamonds." The central areas of the Coulomb diamonds (white in Fig. 1A) correspond to the blockade regime of zero conductance and fixed electron number. Dark stripes parallel to the Coulomb diamond edges in Fig. 1A are peaks in the differential conductance; each stripe represents the transmission resonance of a single QD level aligned with the source or drain Fermi levels (9). For positive V_{DS} we identify the resonances parallel to the negative slope Coulomb diamond edge as unoccupied QD levels in resonance with the source; namely, such peaks correspond to electrons tunneling into subsequent unoccupied states of the QD.

The first evidence of correlations between the excitation spectra of the N - and $(N + 1)$ -electron systems can be seen in Fig. 1B, where the dark stripes of Fig. 1A are visible as multiple resonances on the left edge of each broadened CB peak. Each broadened CB peak shows a tall peak with one, two, three, or four smaller peaks to its left. We identify the tall peak as the first,

second, third, or fourth excited state resonance of the $(N + 3)$, $(N + 2)$, $(N + 1)$, or N -electron system, respectively. At low temperature, $k_B T \ll \Delta$ ($\Delta/k_B T \sim 4$ in our QD) the peak height for each resonance is simply modeled as proportional to the overlap of the wave function in the dot with the source and drain wave functions (16). Thus, the shift of the distinctive tall peak by one position in each successive excitation spectrum suggests that the particular electron wave function associated with this peak and the overall level structure of the QD near the Fermi energy are only weakly perturbed as electrons are removed one by one.

To confirm this correlation between the excitation spectra of adjacent CB peaks, we followed the evolution of each resonance within a broadened CB peak as a function of magnetic field, B . The continuous evolution of the resonance position and height with B yields a distinct signature or "fingerprint" for each quantum level, and collectively for each excitation spectrum. Three broadened CB peaks evolving with B , at fixed V_{DS} , are shown in Fig. 1D. The fingerprints of the N , $(N + 1)$, and $(N + 2)$ excitation spectra display shifted versions of the same level structure; for each electron removed from the dot, one extra level is visible at the top of each spectrum. This shifting agrees with a noninteracting description of the QD in which a fixed spec-

trum is filled one level at a time.

Figure 1C and the energy schemes on the right of Fig. 1D detail the labeling of the QD levels for the data of Fig. 1. The dark stripes of Fig. 1A are identified by color as subsequent QD levels in resonance with the source Fermi level. The energy schemes on the right of Fig. 1D show the state of the system after an electron has tunneled onto the QD from the source and before it has tunneled off to the drain, for the V_G bias that aligns each ground state with the source. Increasing V_G (lowering the dot potential well) brings higher excited states into resonance with the source. For the broadened CB peak separating the $(N - 1)$ and N Coulomb diamonds (red in Fig. 1C) we label these higher resonances as excited states of the N -electron system and show the B field fingerprint of this N excitation spectrum in Fig. 1D. This sequential labeling is understood to be approximately correct [we neglect nonequilibrium effects, which are not resolvable presumably because of thermal broadening (10, 13)]. Negative differential conductance peaks were also observed in our data but will not be described here.

Further understanding of the QD spectral properties was obtained by comparing the fingerprints of ground state addition spectra measured at $V_{DS} = 0$ to that of neighboring excitation spectra, measured at finite V_{DS} .

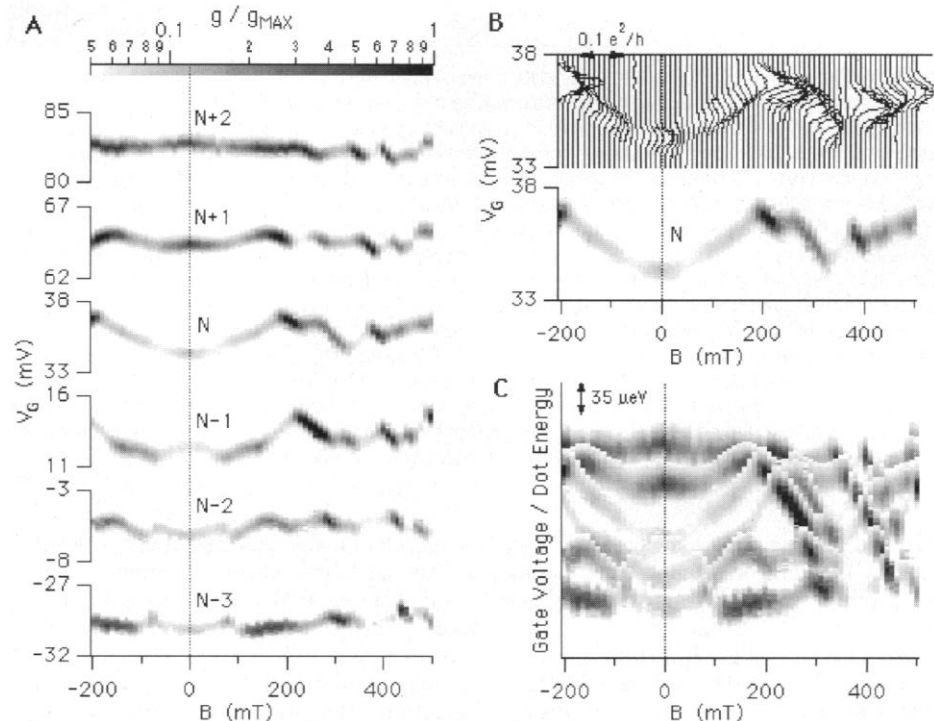


Fig. 2. (A) Six adjacent CB peaks at $V_{DS} = 0$ in gray scale showing both position and height fluctuations as a function of B . The gray scale of g for each trace is normalized to the maximum g of that trace (g_{max}). (B) Trace N shown as raw data and the corresponding gray scale plot. (C) The six traces of (A) are shifted vertically to best align with each other, forming a spectrum with visible anticrossings of adjacent levels.

Six peaks, labeled $(N - 3)$ to $(N + 2)$ in Fig. 2A [where peak N represents the degeneracy between electron numbers N and $(N - 1)$], show the fingerprints of several consecutive ground states. Note that the data in Figs. 2 and 3 are for different surface gate voltages and thus a different QD shape than in Fig. 1. Individual ground states show large peak height and position fluctuations, with the expected symmetry about $B = 0$. In Fig. 2C we collapse this group of levels, originally separated by E_C , by shifting each trace in energy (gate voltage) until they best align with adjacent levels (4). By doing so we assume a Coulomb interaction independent of B . Such translation of the ground states produces a recognizable spectrum coherent over many levels, in which the fluctuations of height and position are visible as anticrossings of neighboring levels. The specific signature of each anticrossing is that two successive levels appear to trade both conductances and velocities $\partial E/\partial B$ as they pass through their point of closest approach (17). This assembled spectrum of fluctuating ground states appears to be composed of slowly varying wave functions as followed through anticrossings, slightly perturbed into the measured anticrossed level structure.

Finally, we compared the assembled ground state spectrum to measured excited state spectra of the same peaks. In Fig. 3, A and B, the N th CB peak at finite bias, showing structure that corresponds to the excited

state spectrum of the N -electron QD, is compared with the N th and $(N + 1)$ th peaks at zero-bias shifted in the same way as in the assembled spectrum of Fig. 2C. It can be seen that the magnetoconductance fingerprint of the N th zero-bias CB peak matches the resonances at both the top and bottom of the N th finite bias CB peak, because all three are identified with the ground state of the N -electron system. More significantly, the $(N + 1)$ th zero-bias CB peak (ground state) matches closely the second resonance (first excited state) of the N th finite bias peak in position, height, and relative spacing between the levels. We emphasize that the observed correspondence between the $(N + 1)$ th ground state and the N th first excited state is trivially implied by a noninteracting electron model but is not obvious in a strongly interacting system.

Despite the overall consistency of the observed addition and excitation spectra with a single-particle picture, there are some important departures that arise presumably as a result of electron-electron interactions. The finite bias structure corresponding to the excited states spectrum of the $(N - 1)$ -electron system is shown in Fig. 3C, whereas Fig. 3D displays the $(N - 1)$ th, N th, and $(N + 1)$ th zero bias peaks shifted in energy from Fig. 2B to best match the $(N - 1)$ excited state spectrum. The relative position of the N th and $(N + 1)$ th levels in Fig. 3D differs considerably from that in Fig. 3B. The $(N + 1)$ th ground state has been

shifted from its alignment of Fig. 3B (same as Fig. 2C) until it is overlapping and even changing places with the N th ground state. This apparent $30\text{-}\mu\text{eV}$ shift of the $(N + 1)$ th level is comparable with the average level spacing of $35\text{ }\mu\text{eV}$ and indicates that although levels may undergo an overall shift in energy as one electron is added, the level “fingerprint” (position and height fluctuations in B) appears largely unchanged. Smaller, similar shifts in level spacings exist in almost all neighboring excitation spectra. Additionally, some resonances show a trend of broadening at higher excited state energies similar to (10).

Another departure from the simple single-particle picture is the absence of spin-degenerate pairs of levels. Previous measurements on few-electron semiconductor QDs (6) and ultrasmall metal QDs (10) showed spin-degenerate level spectra, whereas in-plane magnetic field measurements of a multi-electron semiconductor QD suggested no spin degeneracy (9). In our results the appearance of one new resonance in the excitation spectrum per electron removed from the QD indicates that energy levels in the dot are not spin degenerate. To estimate the energy splitting between spin-paired levels, we examined the spectrum for levels with identical fingerprints. Figure 2B shows that each ground state level has a different fingerprint, implying that none is spin paired. In Fig. 2C, however, some of the slowly varying wave functions followed through anticrossings do appear parallel, suggesting that spin pairing may be visible in this underlying spectrum. We infer in either case that the energy splitting between spin-paired wave functions is larger than the mean single-particle spacing, $\Delta \sim 35\text{ }\mu\text{eV}$. This energy splitting determines the scale of the spin-orbit (18) or electron-electron interaction responsible for the absence of degeneracy.

In conclusion, we have demonstrated that strong correlations exist between the QD energy level spectra of successive electron numbers in the dot, probed by magnetotransport measurements. The excitation spectra of adjacent CB peaks were found to be shifted versions of a very similar spectrum, with the addition of one excited state per electron removed from the dot. These results suggest a single-particle-like picture of level filling, however, with no spin degeneracy. Additional departures from this single-particle model we attribute to electron-electron interactions.

REFERENCES AND NOTES

1. L. P. Kouwenhoven *et al.*, in *Proceedings of the Advanced Study Institute on Mesoscopic Electron Transport*, L. L. Sohn *et al.*, Eds. (Kluwer, Dordrecht, Netherlands, 1997); U. Meirav and E. B. Foxman,

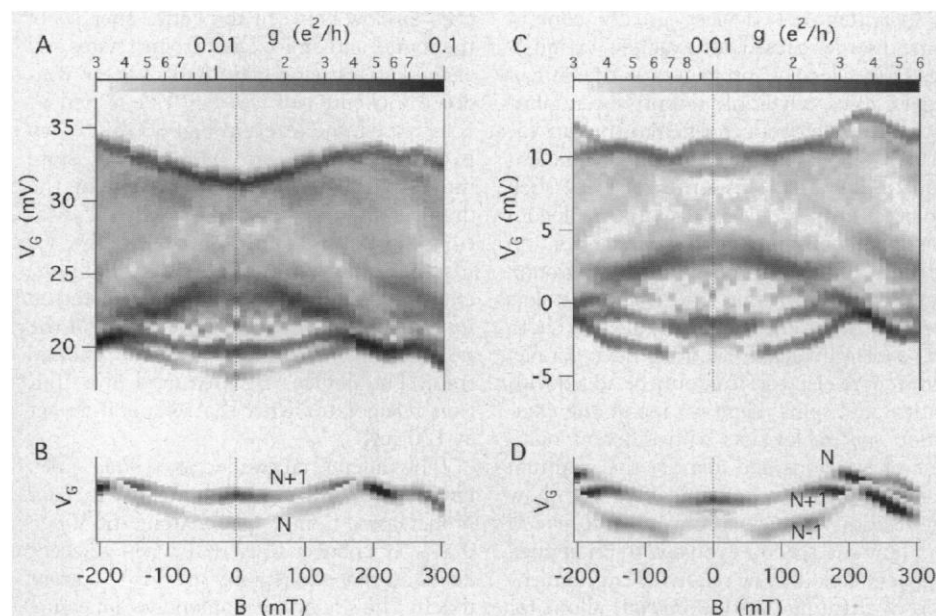


Fig. 3. (A) The magnetic “fingerprint” of the N th CB peak at $V_{DS} = 0.57$ mV. Visible resonances at the bottom of the peak correspond to the excitation spectrum of the N -electron QD. (B) The N th and $(N + 1)$ th zero bias CB peaks, shifted as in Fig. 2C. The N th peak matches both edges of the finite bias peak in (A), and the $(N + 1)$ th peak matches the second resonance (first excited state) in (A). A similar match between the excitation spectrum of the $(N - 1)$ electron system and the $(N - 1)$, N , and $(N + 1)$ ground states is shown in (C) and (D). Note that the relative position of the N th and $(N + 1)$ th peaks is different than in (B).

- Semicond. Sci. Technol.* **10**, 255 (1995).
2. For recent reviews discussing the connection between mesoscopic physics and quantum chaos, see B. L. Altshuler and B. D. Simons, in *Mesoscopic Quantum Physics*, E. Akkermans, G. Montambaux, J.-L. Pichard, J. Zinn-Justin, Eds. (Elsevier, Amsterdam, 1995), pp. 1–98; T. Guhr, A. Mueller-Groeling, H. A. Weidenmueller, <http://xxx.lanl.gov/abs/cond-mat/9707301> (1997); Mesoscopic physics and random matrix theory are discussed in C. W. J. Beenakker, *Rev. Mod. Phys.* **69**, 731 (1997). For a general introduction to quantum chaos, see M. C. Gutzwiller, *Chaos in Classical and Quantum Mechanics* (Springer-Verlag, New York, 1990).
 3. Y. M. Blanter, A. D. Mirlin, B. A. Muzykantskii, *Phys. Rev. Lett.* **78**, 2449 (1997); R. Berkovits and B. L. Altshuler, *Phys. Rev. B* **55**, 5297 (1997).
 4. P. L. McEuen *et al.*, *Phys. Rev. Lett.* **66**, 1926 (1991); P. L. McEuen *et al.*, *Phys. Rev. B* **45**, 11419 (1992).
 5. R. C. Ashoori *et al.*, *Surf. Sci.* **305**, 558 (1994).
 6. S. Tarucha, D. G. Austing, T. Honda, R. J. van der Hage, L. P. Kouwenhoven, *Phys. Rev. Lett.* **77**, 3613 (1996).
 7. A. T. Johnson *et al.*, *Phys. Rev. Lett.* **69**, 1592 (1992).
 8. E. B. Foxman *et al.*, *Phys. Rev. B* **47**, 10020 (1993); P. L. McEuen *et al.*, *Phys. B* **189**, 70 (1993).
 9. J. Weis, R. J. Haug, K. von Klitzing, K. Ploog, *Phys. Rev. Lett.* **71**, 4019 (1993).
 10. D. C. Ralph, C. T. Black, M. Tinkham, *ibid.* **78**, 4087 (1997).
 11. K. Jauregui, W. Häusler, D. Weinmann, B. Kramer, *Phys. Rev. B* **53**, R1713 (1996); D. Weinmann, W. Häusler, B. Kramer, *Phys. Rev. Lett.* **74**, 984 (1995).
 12. D. Pfannkuche and S. E. Ulloa, *Phys. Rev. Lett.* **74**, 1194 (1995).
 13. O. Agam, N. S. Wingreen, B. L. Altshuler, D. C. Ralph, M. Tinkham, *ibid.* **78**, 1956 (1997).
 14. L. P. Kouwenhoven *et al.*, *Science* **278**, 1788 (1997).
 15. C. W. J. Beenakker, *Phys. Rev. B* **44**, 1646 (1991).
 16. _____ and H. van Houten, *Phys. Rev. B* **43**, 12066 (1991).
 17. T. Takami, *Phys. Rev. Lett.* **68**, 3371 (1992).
 18. P. Pfeffer and W. Zawadzki, *Phys. Rev. B* **52**, R14332 (1995).
 19. We thank B. Altshuler, D. Ralph, and M. Heiblum for useful discussions and S. Patel and A. Huibers for valuable help throughout the measurements. We acknowledge support from Joint Services Electronics Program under grant DAAH04-94-G-0058, the Army Research Office under grant DAAH04-95-1-0331, the Office of Naval Research Young Investigator program under grant N00014-94-1-0622, and the NSF–National Young Investigator program. D.S. acknowledges the support of MINERVA grant.

19 September 1997; accepted 5 November 1997

Excitation Spectra of Circular, Few-Electron Quantum Dots

L. P. Kouwenhoven, T. H. Oosterkamp, M. W. S. Danoesastro, M. Eto, D. G. Austing, T. Honda, S. Tarucha

Studies of the ground and excited states in semiconductor quantum dots containing 1 to 12 electrons showed that the quantum numbers of the states in the excitation spectra can be identified and compared with exact calculations. A magnetic field induces transitions between the ground and excited states. These transitions were analyzed in terms of crossings between single-particle states, singlet-triplet transitions, spin polarization, and Hund's rule. These impurity-free quantum dots allow "atomic physics" experiments to be performed in magnetic field regimes not accessible for atoms.

Small solid-state devices known as quantum dots are often referred to as artificial atoms because their electronic properties resemble, for example, the ionization energy and discrete excitation spectrum of atoms (1). Quantum dots are usually fabricated between source and drain contacts so that the atomlike properties can be probed in current-voltage (I - V) measurements. Additionally, with a gate electrode nearby, the exact number of electrons N can be varied on the quantum dot by changing the gate voltage V_g . When an electron is added, the total charge on the dot changes by the elementary charge e . The associated energy change, known as the addition energy, is a combination of the single-electron charging energy and the change in single-particle energy. Charging effects and discrete single-particle states have been studied in a variety of quantum dot systems, defined not only in

semiconductors but also in metal grains and molecules (2).

Quantum dot devices usually contain some disorder caused, for example, by impurities (2). Clean quantum dots, in the form of regular disks, have only recently been fabricated in a semiconductor heterostructure (3, 4). The circular symmetry of the two-dimensional (2D) disks gives rise to a 2D shell structure in the addition energies, analogous to the 3D shell structure in atomic ionization energies (5). Measurements of the ground states have shown that the 2D shells in dots are filled according to Hund's rule (4): Up to half-shell filling, all electrons have parallel spins; more electrons can only be added with antiparallel spins. Here we report the excitation spectra for dots with different numbers of electrons and identify the quantum numbers of the excited states. We also show the relation between spectra of successive N and how the spectra evolve with an applied magnetic field B . The relatively large dimension of quantum dots (~ 100 nm) allows for the use of accessible B fields that would correspond in real atoms to inaccessible fields of the order 10^6 T.

The device consists of, from bottom to top, an n -doped GaAs substrate; undoped layers of $\text{Al}_{0.22}\text{Ga}_{0.78}\text{As}$ (7.5 nm thick), $\text{In}_{0.05}\text{Ga}_{0.95}\text{As}$ (12 nm thick), and $\text{Al}_{0.22}$

$\text{Ga}_{0.78}\text{As}$ (9.0 nm thick); and a top layer of n -doped GaAs (~ 500 nm thick) (Fig. 1A). A submicrometer pillar is fabricated by electron-beam lithography and etching techniques (3). Source and drain wires are connected to the top and substrate contacts, and a third wire is attached to the metal side gate that is placed around the pillar. The energy landscape is shown in Fig. 1B. The AlGaAs layers are insulating, but thin enough to allow for tunneling from the source to the drain through the central, disk-shaped InGaAs layer. If V_g is made more negative, the effective diameter of this disk can be reduced from a few hundred nanometers down to zero, decreasing N one by one from ~ 70 to zero. At a particular V_g , the excitation spectrum can be probed by increasing the source-drain voltage, V_{sd} , which opens up a transport window between the Fermi energies of the source and drain. Only ground states and excited states lying within this energy window contribute to I (see Fig. 1B). When V_g is increased, the levels in Fig. 1B shift down in energy; when an extra energy state moves through the Fermi energy of the drain, I increases. Unlike atoms, excitations do not occur inside the dot by, for instance, absorption of radiation. For dots, excitations are created when an electron tunnels out from the ground state and the next electron tunnels into an excited state. The devices are measured in a dilution refrigerator with the temperature set at 100 mK.

The differential conductance $\partial I / \partial V_{sd}$ as a function of V_{sd} and V_g is shown in Fig. 2 for N increasing from 0 to 12. Along the $V_{sd} \approx 0$ axis, N changes to $N + 1$ when adjacent diamond-shaped regions of zero current touch. The size of the diamonds is a measure of the minimum energy to add or subtract an electron. The diamonds for $N = 2, 6,$ and 12 are unusually large, which correspond to filled shells (4). At the two upper edges of the N electron diamond, an extra electron can tunnel through the dot via the $N + 1$ electron ground state. Excited states of the N

L. P. Kouwenhoven, T. H. Oosterkamp, M. W. S. Danoesastro, Department of Applied Physics and Delft Institute of MicroElectronics and Submicrontechnology, Delft University of Technology, Post Office Box 5046, 2600 GA Delft, Netherlands.

M. Eto, Department of Physics, Faculty of Science and Technology, Keio University, 3-14-1 Hiyoshi, Kohoku-ku, Yokohama 223, Japan.

D. G. Austing, T. Honda, S. Tarucha, NTT Basic Research Laboratories, 3-1, Morinosoto Wakamiya, Atsugi-shi, Kanagawa 243-01, Japan.